PERGAMON

Electrochimica Acta 45 (2000) 2289–2296

ELECTROCHIMICA Acta

www.elsevier.nl/locate/electacta

Electrocatalytic activity of ruthenium for oxygen reduction in alkaline solution

Jai Prakash *, Humberto Joachin

Center for Electrochemical Science and Engineering, Department of Chemical and Environmental Engineering, Illinois Institute of Technology, 10 W 33rd Street, Chicago, IL 60616, USA

Received 5 November 1999

Abstract

The electrochemical behavior and the electrocatalytic activity of ruthenium electrode for oxygen reduction are examined using cyclic voltammetry and rotating ring-disk electrode techniques. A surface oxide film on ruthenium metal is formed when the potential is scanned in the positive direction of hydrogen adsorption and evolution region. This oxide film affects the activity of ruthenium for oxygen reduction reaction. Oxygen reduction on ruthenium electrode proceeds primarily by a direct 4-electron reduction pathway without producing significant amounts of solution phase peroxide. The kinetic results suggest the initial electron transfer as the rate-determining step.

Keywords: Ruthenium; Oxygen reduction; Kinetics; Tafel plots; Cyclic voltammetry; Rotating ring-disk electrode

1. Introduction

Owing to the technological significance of the ruthenium and ruthenium oxide, a large number of studies on the electrochemical properties of ruthenium and its activity towards oxygen reduction [1–25] have been extensively reported in literature. Despite these studies of the oxygen electrode reactions, the mechanistic aspects are still not very well understood due to the complex electrochemical behavior of ruthenium metal. It has been generally accepted that the nature of the electrode material is one of the important variables in the oxygen reduction process. It has also been argued in literature that the oxide coverage [18] and rest potential [19] strongly depend on the d-band character of the electrode material. The complex electrochemical behavior of ruthenium electrode towards the oxygen reaction, therefore, is attributed to the adsorption characteristics of hydrogen and oxygen on this metal [8,9], the difficulties in the interpretation of the current-potential curves [15], and relatively low corrosion resistance at anodic potentials [25]. Besides these problems, the surface oxidation of Ru begins at a very low potential (ca. +0.25 V versus RHE) before the end of hydrogen desorption leading to an overlap on these two processes. Even for the oxygen reduction process, ruthenium electrode is covered with a hydrated oxide film. The degree of oxidation of the electrode surface has a considerable influence on the kinetics of O_2 reduction reaction since the thickness and structure of this oxide film are both time and potential dependent. An excellent study on the oxygen reduction reaction on ruthenium electrode in alkaline solution has been described by Adzic et al. [10]. However, a comparison of the oxygen reduction in the forward and backward directions and the effect of solution pH on this reaction are not reported. This paper describes the O_2 reduction on the ruthenium electrode in alkaline solution based on the ring-disk electrode studies. The effects of the for-

* Corresponding author. Fax: +1-312-5678874.
E-mail address: prakash@charlie.cns.iit.edu (J. Prakash)

0013-4686/00/$ - see front matter
PII: S0013-4686(99)00439-9

ward and backward scans and solution pH on the kinetic aspects of the oxygen reduction are also examined.

2. Experimental

The experiments were carried out in an all-Teflon cell with a main compartment for the working electrode and two separate small compartments for the counter and reference electrodes plus a Luggin capillary for the latter in order to minimize IR drop. The oxygen reduction measurements were carried out using the interchangeable ring-disk electrode assembly (Model AFDTI36, Pine Instrument Co., Grove City, PA) with a collection efficiency of 0.22. The ring was made of gold. The disk consisted of a Ru rod, 99.999%, 5 mm diameter × 11 mm (Metal Crystals Ltd., Cambridge, UK) embedded in a Teflon holder and mounted into the interchangeable ring-disk assembly. Successive stages of mechanical polishing of the electrode were carried out with the silicon carbide paper (600 grit, 3M Co.), emery grinding papers (0, 00, 0000 grits, Buehler Ltd.), and 0.05 μm γ-alumina powder (Buehler Ltd.). While polishing the electrode was inserted into a Teflon holder to keep it vertical. A Buehler microcloth was used for polishing with alumina and ultrapure water was used as a lubricant and wash. After a mirror finish was achieved, the electrode was cleaned ultrasonically in ultrapure water to remove alumina particles. For subsequent experiments, only polishing with water-paste of 0.05 μm γ-alumina was repeated and the surface then cleaned ultrasonically.

The electrolyte, 0.1 M KOH solutions, was prepared from 50% NaOH solution (Fisher Scientific, low in carbonate). The potentiostat used for the ring-disk measurements was a Pine RDE-3 bipotentiostat (Pine Instrument) with a built-in sweep generator. A gold foil was used as a counter electrode and Hg/HgO, 0.1 M OH^- as the reference electrode. The ring was typically set at +0.15 V versus Hg/HgO, OH^- to oxidize peroxide at the mass transport limited rate. Before recording the ring currents, however, the ring was activated by stepping the ring potential from +0.15 to −0.60 V for 1 min to reduce the oxide film and then back to +0.15 V at each rotation.

3. Results and discussion

3.1. Cyclic voltammetry

Fig. 1 shows the voltammogram obtained by increasing the anodic potential limit. The cathodic potential limit has been chosen at −0.90 V (Hg/HgO, OH^-) in order to avoid the hydrogen generation reaction as far as possible. The cyclic voltammetric behavior of ruthenium is consistent with the studies reported in literature [6,7,10,26]. The anodic curves in Fig. 1 after the hydrogen evolution region represent the oxidation of the ruthenium surface followed by the reduction of the oxide in the cathodic direction. The oxidation of the ruthenium surface starts just after hydrogen evolution followed by a broad peak in the anodic potential. It can be seen from the cyclic voltammogram of ruthenium that the rate of the oxide reduction depends on the anodic limit [17]. It is observed that the oxide formed during the anodic sweep starting from hydrogen evolution to about −0.3 V versus Hg/HgO is reversibly chemisorbed. However, increasing the anodic potential makes the surface oxide progressively irreversible in that higher cathodic potentials are required to reduce the oxide film [7,10]. According to Pourbaix [27], the formation of the oxide on the Ru metal in alkaline solution (0.1 M KOH) does not occur until 0.0 V versus Hg/HgO and therefore no formation of oxide should be

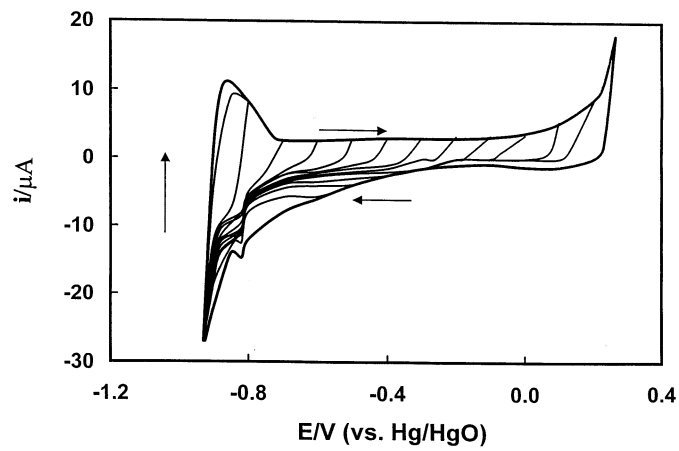

Fig. 1. Cyclic voltammetry for the ruthenium electrode in Ar-saturated 0.1 M KOH. Electrode area: 0.196 cm^2; scan rate: 10 mV/s.

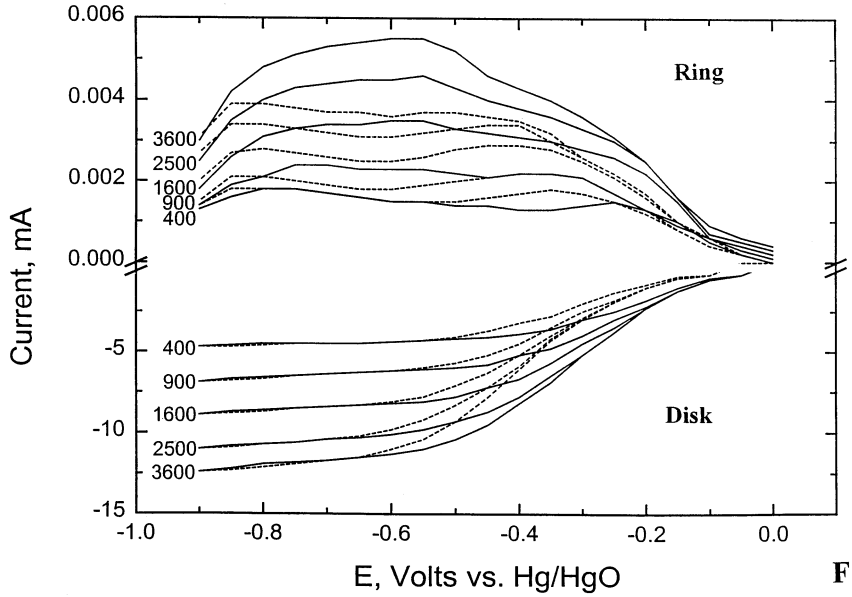

Fig. 2. Rotating ring-disk currents for oxygen reduction on Ru electrode in O_2 saturated 0.1 M KOH at 25°C. Disk electrode area: 0.196 cm^2. Collection efficiency: 0.22. Ring potential: 0.15 V versus Hg/HgO. Scan rate: 10 mV/s. Dotted lines represent the measurements for the disk potential scan from −0.9 to 0.0 V. Solid lines represent the measurements for the disk potential scan from 0.0 to −0.9 V.

expected to occur at potentials negative to 0.0 V versus Hg/HgO. However, it has been found that the surface oxide on ruthenium is not completely reduced even at potentials well below this value. Similar behavior has also been reported on other noble metal electrodes. On platinum electrode, for example, it has been shown [28] that the first 15% of the surface monolayer oxide can be reversibly reduced during the cathodic scan. Increasing the oxide coverage beyond 15% of the monolayer, however, requires higher cathodic potentials. Gold, on the other hand, is very similar to ruthenium in the sense that the irreversible oxidation of the electrode surface starts at very early stages of the surface oxidation. On gold electrode, for example, even at a surface coverage of 2% of the monolayer, the oxide cannot be reversibly reduced [29]. Conway et al. [29] explained this effect by 'place exchange' or the rearrangement of the surface layer to a 2-dimensional lattice of 'O' species amongst metal atoms. This rearranged layer has also been suggested [29] to be thermodynamically more stable than the chemisorbed ad-layer in order to explain the irreversible oxidation of the electrode surface at increasing anodic potentials. The cyclic voltammetric behavior of ruthenium electrode can also be explained based on the irreversible surface oxidation at early anodic potential followed by the surface rearrangement. The surface layer formed during the anodic oxidation of ruthenium can be visualized to be composed of oxygen containing species, which are probably formed by the discharge of the water molecule in aqueous solutions. The formation of the oxide film is probably initiated by the discharge of water molecules to give a hydrated surface at potentials < 0.0 V versus Hg/HgO, which then undergoes further reactions with increasing anodic potentials.

3.2. Oxygen reduction

The polarization curves for O_2 reduction on Ru at a series of rotation rates are shown in Fig. 2. Before taking these polarization curves, the Ru disk was cycled into the hydrogen adsorption region, i.e. between the potential limits −0.9 to −0.7 V. It can be seen from this figure that the ring current, which corresponds to the diffusion-controlled oxidation of peroxide, shows complex behavior. These currents are very small indicating the O_2 reduction on the disk involving close to four electrons per O_2 molecule. The ring current increases with increasing potential, reaches a maximum at ca. −0.056 V, and subsequently decreases. This maximum, however, is not clearly visible at lower rotation rates. The change in the disk current, however, is very small even at the potential corresponding to the maximum ring current (Fig. 2). Consequently, the principal reaction at the disk electrode continues to involve the 4-electron overall reduction. For a rotating disk electrode experiment involving an electrode process, which is first order in reactant, the observed current is expressed by [30]

$$\frac{1}{i}=\frac{1}{i_k}+\frac{1}{i_L} \quad (1)$$

where i_k is the kinetic current and i_L is the diffusion limiting current. An expression for i_L is given by

$$i_L = Bf^{1/2} \quad (2)$$

where f is the rotation rate and B can be expressed by

$$B = 0.62nFAC_{O_2}(D_{O_2})^{2/3}\,v^{-1/6} \quad (3)$$

where n is the overall number of electrons transferred, F is the Faraday constant, A is the electrode area, C_{O_2} is the bulk concentration of O_2, D_{O_2} is the diffusion coefficient for O_2, and v is the kinematic viscosity of the electrolyte. A plot of $1/i$ versus $1/\sqrt{f}$ for various potentials should yield straight lines with intercept corresponding to i_k and the slopes yielding the B values. Such plots are shown in Figs. 3 and 4 for forward (from -0.9 to $+0.0$ V) and backward (from $+0.0$ to -0.9 V) scans. B values were experimentally determined from the slopes of the plots in Figs. 3 and 4. The slope remains nearly constant over the potential range -0.7 to -0.3 V indicating a constant value of number of electrons transferred for the O_2 reduction on the Ru disk electrode for both the forward and the backward scans. The experimental value of B (0.023 mA (rpm)$^{-1/2}$) agrees reasonably well with the theoretical value (0.025 mA (rpm)$^{-1/2}$) calculated from Eq. (3) using literature data for the O_2 solubility [31], diffusion coefficient [31] and kinematic viscosity [32] of the electrolyte. The values of B were observed to remain almost constant for both forward and backward scans over the potential range -0.30 to -0.70 V, indicating a constant value of $n = 3.7$ for the O_2 reduction.

The parallel linear i^{-1} versus $f^{-1/2}$ plots in Figs. 3 and 4 for the forward and the backward scan provide support for a first order reaction with respect to O_2. The mass transport corrected Tafel plots of log $i_L \cdot i/(i_L - i)$ versus E for the forward and backward scans are shown in Fig. 5. The Tafel lines reaching sort of a plateau at about -0.6 V in Fig. 5 can be explained by the fact that the disk currents reach close to the limiting current values at potentials cathodic to -0.6 V. This results in negligible change in the mass transport corrected disk currents with potential cathodic to -0.6 V as shown in Fig. 5. The mass transport correction was made using the limiting current, $i_L = B\sqrt{f}$, where f is the rotation rate. A Tafel slope of -165 mV/decade is observed in the linear region for the forward scan, i.e. when the electrode is scanned from -0.9 to $+0.0$ V, while the Tafel slope of -250 mV/decade is observed for the backward sweep ($+0.0$ to -0.8 V). This clearly means that the oxygen reduction on the two surfaces is very different. The change in the Tafel slopes in the forward and the backward reactions is a result of the significantly large hysteresis effects observed when the sweeps were reversed. This phenomenon may be explained on the basis of two different surfaces involved in the process. The polarization curve in the forward direction represents the O_2 reduction on somewhat less oxidized electrode surface, since some of the surface oxide has been reduced during cycling in the hydrogen adsorption region. However, when the polarization curve is recorded in the back direction, the electrode surface has relatively thicker layer of oxide than in the forward scan, as a result of which there is

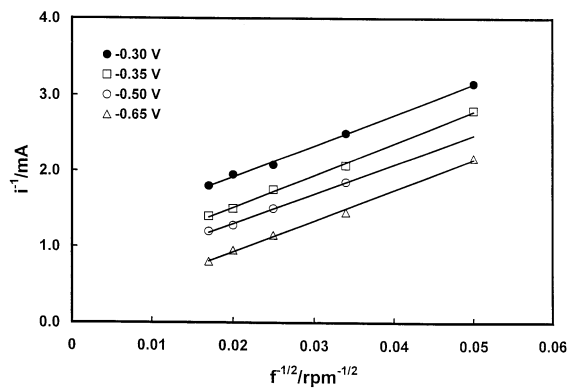

Fig. 3. i^{-1} versus $f^{-1/2}$ plots for the O_2 reduction on Ru at various disk potentials for the forward scan.

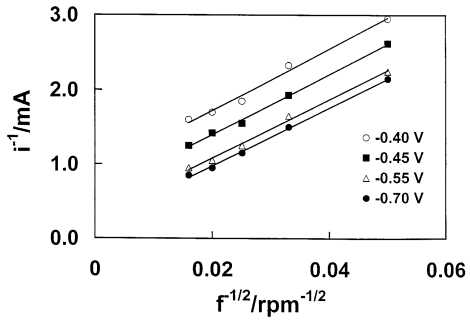

Fig. 4. i^{-1} versus $f^{-1/2}$ plots for the O_2 reduction on Ru at various disk potentials for the backward scan.

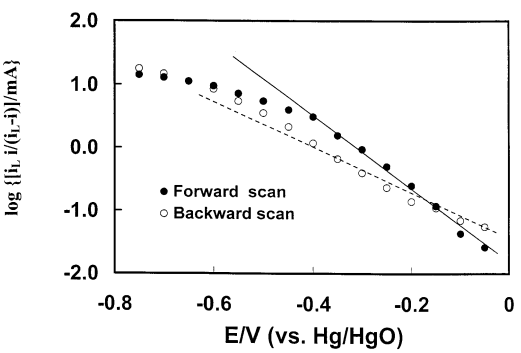

Fig. 5. Tafel plots for the O_2 reduction on Ru at 25°C constructed from the data in Fig. 5.

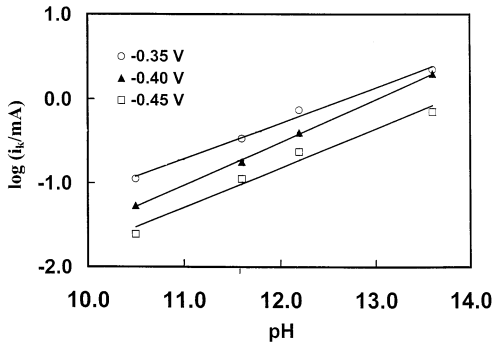

Fig. 6. Dependence of the kinetic current for the O_2 reduction on pH for a Ru rotating disk electrode in O_2-saturated KOH solutions.

considerable change in the polarization curves. Meyer [33] has explained the high values of the Tafel slope (≥ -120 V/decade) and fractional orders for O_2 reduction on zirconium on the basis of the charge transfer through the ZrO_x film. In the case of Ru, the oxidation of the surface starts at an earlier stage than other noble metals. This surface oxide film has been shown to be potential and time-dependent [15] with oxide penetrating the ruthenium metal [34]. However, the RuO_x film on Ru has much higher conductivity [35] than ZrO_x on Zr or PtO_x on Pt. Therefore, the dual layer model involving the subsurface oxygen and the IR drop in the oxide layer seems to be less probable mechanism to explain the high value of the Tafel slope. However, the value of the slope in this study is, however, sensitive to the thickness and structure of the oxide film as is evident from the different values of the Tafel slope for the forward and backward sweeps. One reasonable explanation may be that the oxygen reduction is under mixed kinetic and diffusion controlled as explained by Nekrasov and Khruscheva [24].

The effect of pH on the kinetic currents is shown in Fig. 6. It was observed that decreasing the pH shifts the onset of O_2 reduction to more cathodic potentials. Fractional orders were obtained with respect to pH but the order was not reproducible in our experiments. The fractional orders with respect to pH for oxygen electrode reactions are not uncommon in literature [36–39]. However, for an oxide-covered surface, the determination of the reaction order with respect to hydroxide activity presents some problems for an oxide–electrolyte solution interface. The evaluation of the reaction order requires that the voltage drop between the outer Helmholtz plane in the oxide and that of the electrolyte phases, $(\phi_2)_{\text{oxide}} - (\phi_2)_{\text{electrolyte}}$ be held constant. The potential distribution across the interface, however, is dependent on the pH. Therefore, while the voltage drop between the bulk phases can be held constant through the use of a potentiostat, $(\phi_2)_{\text{oxide}} - (\phi_2)_{\text{electrolyte}}$ is likely to vary. Trassati et al. [36,37] explained the fractional order based on the surface acid-base dissociation of oxidized sites whose concentration ratio depends on pH. The fractional order obtained in this study can also be explained by the mechanism suggested by Trassati et al. [36,37] in view of the oxidized ruthenium surface present during the reduction reaction.

Kinetic analysis of the ring-disk data was carried out using the method of Wroblowa [40] as shown below.

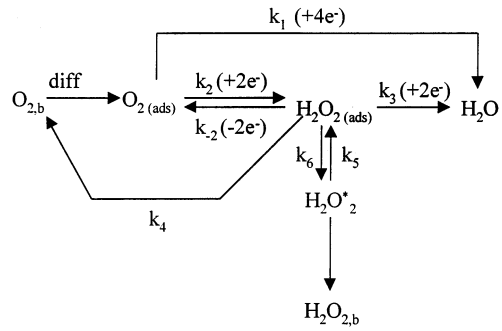

From this scheme the rate of the disk to ring current is given as

$$N\frac{i_D}{i_R} = 1 + \frac{2k_1}{k_2} + A + \frac{A \cdot k_6}{Zf^{1/2}} \tag{4}$$

where N is the collection efficiency, $Z = 0.62\ D^{2/3}\ v^{-1/6}$ and

$$A = \frac{k_1}{k_2 k_5} \cdot (k_2 + k_3 + k_6) + \frac{(2k_3 + k_4)}{k_5} \tag{5}$$

for the series mechanisms only, i.e. when $k_1 = 0$, equation reduces to

$$N\frac{i_D}{i_R} = 1 + \frac{2k_3 + k_4}{k_5} + \frac{k_6}{Zf^{1/2}}\frac{(2k_3 + k_4)}{k_5} \tag{6}$$

This equation provides diagnostic criteria in distinguishing the series and parallel pathways for the O_2 reduction reaction [40–44]. Figure 7 shows the plots of $N(i_D/i_R)$ versus $1/f^{1/2}$. It can be seen from this figure that the plots yield straight lines and intercepts that are greater than unity and potential dependent.

Eq. (4), however, predicts that the slopes and intercepts obtained at various potentials from the $N(i_D/i_R)$ versus $1/f^{1/2}$ plot are related by the equation

$$J = 1 + \frac{2k_1}{k_2} + \frac{SZ}{k_6} \tag{7}$$

where J is the intercept and S is the slope. If k_1 and k_2 have the same potential dependence and the adsorption–desorption rate constants k_5 and k_6 are assumed to depend little on potential, equation predicts a linear relationship between J and S with the intercept depending on the ratio of k_1 and k_2. Figure 8 shows such a

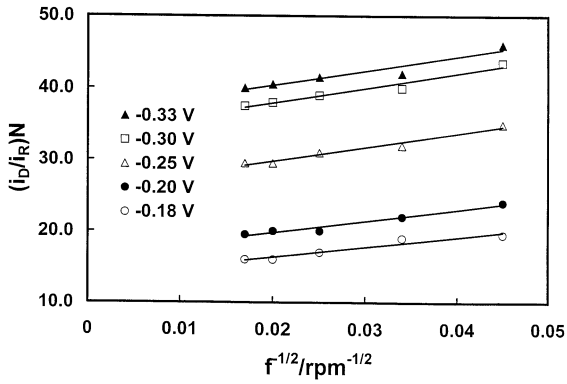

Fig. 7. $(i_D/i_R)N$ versus $f^{-1/2}$ plots for the O_2 reduction on Ru electrode in 0.1 M KOH at various disk potentials. Data are taken from Fig. 2.

plot. From the intercept of the plot, it was found that $k_1 = 6k_2$.

3.3. Discussion of mechanism

A Tafel slope of -165 mV/decade suggests that the initial 1-electron transfer is the rate-determining step. The results of the rotating disk experiments suggest that at potentials below -0.5 V the oxygen reduction occurs via direct 4-electron reduction. Since, the ruthenium electrode surface is in oxidized form, a direct 4-electron reduction on ruthenium electrode seems to be less plausible because the oxygen reduction on the oxidized electrode surfaces of the noble metals has been shown to produce H_2O and H_2O_2 [45,46]. Based on the ellipsometry data [34], Anastasijevic et al. [5,10,11] have suggested the existence of Ru sites on the oxidized surface based on a 'sandwich' type structure with Ru/O/Ru composition. They explained the oxygen reduction via the formation of O–O bridge with the surface ruthenium atoms followed by the bond rupture. The side-on adsorption of oxygen to form O–O bridge on the electrode surface requires proper spacing of the ruthenium atoms on the surface in order for them to participate in bonding interactions with the oxygen molecule. It has been proposed [10] that the place exchange of O and Ru brings ruthenium atoms on the electrode surface in order to facilitate the O–O bridge formation. However, the orientation of all of the ruthenium sites at an optimum distance on the oxidized electrode surface to allow for a side-on adsorption [10,11] of all of the O_2 molecules seems to be less probable. Since, the O_2 reduction on ruthenium takes place predominantly by 4-electron reduction to water, we propose that the oxygen reduction takes place on the similar electrode surface as proposed by Anastasijevic et al. [10]. However, the oxygen adsorption probably involves a single ruthenium atom per oxygen molecule. The involvement of a single ruthenium site per oxygen molecule does not impose the strict conditions of optimum placement of ruthenium atoms as required for a side-on adsorption involving two ruthenium sites.

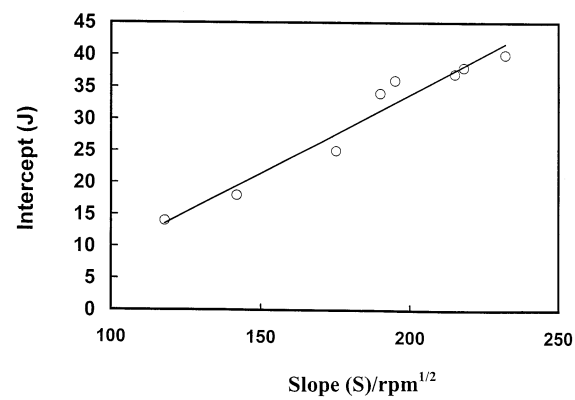

Fig. 8. J versus S plots for the O_2 reduction on Ru electrode in 0.1 M KOH. The values of J and S are obtained from the intercepts and slopes of the lines in Fig. 7.

Since the surface of the RuO_x on Ru electrode is negatively charged under the experimental conditions of this study and does not favor the adsorption of negatively charged O_2 species, the oxygen molecules adsorb on the electrode surface followed by a slow first electron transfer. The interaction of this adsorbed oxygen species on the ruthenium metal involves a lateral interaction of the dz^2 orbitals of ruthenium metal and π orbitals of the superoxide ion with back bonding from at least partially filled d_{xy} or d_{yz} orbitals of Ru to the π^* orbitals of the oxygen species [47]. The Vaska complexes [48] such as $Ir(O_2)Cl(CO)(PPh_3)_2$ appear to form such complexes with O_2 [49]. These compounds are selective oxidation catalysts for cyclic olefins [50]. This interaction results in an increase in O–O bond length due to strong metal–oxygen interaction and consequently the rupture of O–O bond giving rise to 4-electron reduction of O_2. The following steps may occur for the O_2 reduction on Ru with Eq. (9) as the rate-determining step.

$$N\frac{i_D}{i_R} = 1 + \frac{2k_1}{k_2} + A + \frac{A \cdot k_6}{Z f^{1/2}}$$

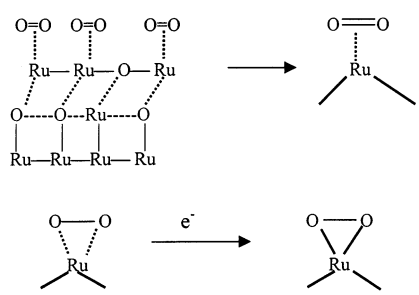

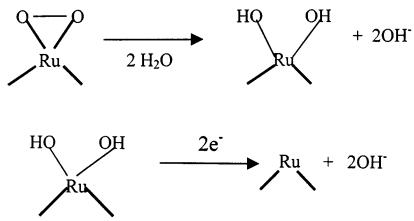

The cooperative interaction of the oxygens with the protons of H_2O may reduce the stability of the O–O bond and eventually dissociate the bond as shown in Eq. (11). The further reduction of the species generated in step 11 is analogous to the reduction of the oxide film Ru-OH. Since the O_2 reduction measurements are carried out in the potential range -0.7 to -0.3 V, the species $Ru(OH)_2$ generated in Eq. (11) can be reduced further as shown in Eq. (12) to yield four electrons overall for O_2 reduction on Ru.

4. Conclusions

Cyclic voltammetry of the ruthenium metal shows that an oxide film on Ru metal is formed when the potential is scanned in the positive direction of hydrogen adsorption and evolution region. This film is reduced when the sweep is reversed. This oxide film affects the activity of Ru metal for oxygen reduction reaction. The rotating ring-disk experiments show that although the reduction proceeds by 4-electron pathway, the kinetics and mechanism depend on the oxidation state of the Ru surface. A Tafel slope of -165 mV/decade was observed in the linear region for the forward scan (-0.9 to $+0.0$ V), while the Tafel slope of -250 mV/decade is observed for the backward sweep ($+0.0$ to -0.8 V). These results suggest that the oxygen reduction on the two surfaces is very different and is explained on the basis of two different surfaces involved in the process. The kinetic results also indicate the first electron transfer as the rate-determining step for the oxygen reduction on the ruthenium electrode.

Acknowledgements

This work was supported by the Chemical Technology Division of the Argonne National Laboratory. The authors are grateful to Dr Jim Miller, Dr Donald Vissers, and Dr Khalil Amine of the Chemical Technology Division, Argonne National Laboratory for encouragement and support.

References

[1] S. Trassati, W.E. O'Grady, in: H. Gerischer, C.W. Tobias (Eds.), Advances in Electrochemistry and Electrochemical Engineering, vol. 12, Wiley, New York, 1981, p. 177.
[2] L.D. Burke, in: S. Trasatti (Ed.), Electrodes of Conductive Metallic Oxides (part A, ch. 3), Elsevier, Amsterdam, 1980, p. 41.
[3] L.D. Burke, M.K.G. Lyons, in: R.E. White, J. O'M Bockris, B.E. Conway (Eds.), Modern Aspects of Electrochemistry (no. 18, ch. 4), Plenum, New York, 1986, p. 169.
[4] E.J.M. O'Sullivan, E.J. Calvo, in: R.G. Compton (Ed.), Chemical Kinetics, vol. 27, Elsevier, Amsterdam, 1987, p. 247.
[5] N.A. Anastasijevic, Z.M. Dimitrijevic, R.R. Adzic, Electrochim. Acta 37 (1992) 457.
[6] M. Vukovic, J. Chem. Faraday Trans. 86 (22) (1990) 3743.
[7] M. Vukovic, Electrochim. Acta 34 (1989) 287.
[8] D. Michell, D.A.J. Rand, R. Woods, J. Electroanal. Chem. 89 (1978) 11.
[9] D. Galizzoli, F. Tantardini, S. Trasatti, J. Appl. Electrochem. 4 (1974) 57.
[10] N.A. Anastasijevic, Z.M. Dimitrijevic, R.R. Adzic, J. Electroanal. Chem. 199 (1986) 351.
[11] N.A. Anastasijevic, Z.M. Dimitrijevic, R.R. Adzic, Electrochim. Acta 31 (1986) 1125.
[12] J.P. Hoare, The Electrochemistry of Oxygen, Interscience, 1968.
[13] S. Hadzi-Jordanov, H. Angerstein-Koslowaka, M. Vukovic, B.E. Conway, J. Phys. Chem. 81 (1977) 2271.
[14] M Vukovic, H. Angerstein-Koslowaka, B.E. Conway, J. Appl. Electrochem. 12 (1982) 193.
[15] S. Hadzi-Jordanov, H. Angerstein-Koslowaka, M. Vukovic, B.E. Conway, J. Electrochem. Soc. 125 (1978) 1471.
[16] L.D. Burke, J.K. Mulcahy, S. Venkatesan, J. Electroanal. Chem. 81 (1977) 339.
[17] L.D. Burke, J.K. Mulcahy, J. Electroanal. Chem. 73 (1976) 207.
[18] M.L.B. Rao, A. Damjanovic, J. O'M Bockris, J. Phys. Chem. 67 (1963) 2508.
[19] J.P. Hoare, Electrochim. Acta 14 (1969) 797.
[20] G. Iwakura, K. Hirao, H. Tamura, Electrochim. Acta 22 (1977) 335.
[21] A. Damjanovic, J. O'M Bockris, J. Electroanal. Chem. 6 (1966) 401.
[22] L.D. Burke, O.J. Murphy, J. Electroanal. Chem. 96 (1979) 19.
[23] L.D. Burke, O.J. Murphy, J. Electroanal. Chem. 109 (1980) 199.
[24] L.N. Nekrasov, E.I. Khruscheva, Elektrokhimiya 3 (1967) 166.
[25] V.V. Gorodetskii, M.M. Pecherskii, Ya B. Skuratnik, M.A. Dembrovskii, V.V. Losev, Elektrokhimiya 9 (1973) 894.
[26] L.N. Velikodnyi, V.A. Shepelin, E.V. Kasatkin, G.I. Zagryadskaya, Electrokhimiya 17 (1981) 1397.
[27] M. Pourbaix, Atlas of Electrochemical Equilibria in Aqueous Solutions, Pergamon Press, Oxford, 1966, pp. 343–349.

[28] S.B. Brummer, J.I. Ford, M.J. Turner, J. Phys. Chem. 69 (1965) 3424.
[29] B.E. Conway, E. Gilieadi, M. Dzieciuch, Electrochim. Acta 8 (1963) 143.
[30] V.G. Levich, Physicochemical Hydrodynamics, Prentice Hall, Englewood Cliffs, NJ, 1962.
[31] R. Davis, G. Horvath, C.W. Tobias, Electrochim. Acta 12 (1967) 287.
[32] CRC Handbook of Chemistry and Physics, 65th edn., CRC Press, Florida, 1984.
[33] R.E. Meyer, J. Electrochem. Soc. 107 (1960) 847.
[34] L.N. Velikodnii, V.A. Shefelin, E.V. Kasatkin, Elektrokhimiya 18 (1982) 1275.
[35] S. Trasatti, G. Lodi, in: S. Trasatti (Ed.), Electrodes of Conductive Metallic Oxides, Part A, Elsevier, Amsterdam, 1981, p. 301.
[36] C. Angelinetta, M. Falciola, S. Trasatti, J. Electroanal. Chem. 205 (1986) 347.
[37] A. Carugati, G. Lodi, S. Trasatti, Mater. Chem. 6 (1981) 255.
[38] D.V. Kokoulina, Yu I. Krasovitskaya, T.V. Ivanova, Elektrokhimiya 14 (1978) 470.
[39] L.I. Krishtalik, Electrochim. Acta 26 (1981) 329.
[40] H.S. Wroblowa, Y.D. Pan, G. Razumney, J. Electroanal. Chem. 60 (1976) 195.
[41] A. Damjanovic, M.A. Genshaw, J. O'M Bockris, J. Electroanal. Chem. 15 (1967) 173.
[42] V.S. Bagotskii, V. Yu Filinovskii, N.A. Shumilova, Elektrochimiya 4 (1968) 1247.
[43] M.R. Tarasevich, Elektrochimiya 4 (1968) 210.
[44] R.W. Zurrilla, R.K. Sen, E.B. Yeager, J. Electrochem. Soc. 125 (1978) 1103.
[45] V.J. Lukyanycheva, A.V. Yuzhenina, A.J. Lentsner, L.L. Knots, N.A. Ahunilova, V.S. Bagotskii, Elektrokhimiya 7 (1971) 1287.
[46] M.R. Tarasavich, V.S. Vilinskaya, Elektrokhimiya 9 (1973) 96.
[47] J.S. Griffith, Proc. R. Soc. (A) 235 (1956) 23.
[48] L. Vaska, Science 140 (1963) 809.
[49] J. McGinnety, R. Doedens, J. Ibers, J. Am. Chem. Soc. 88 (1966) 3511.
[50] J. Collman, M. Kubola, J. Hosking, J. Am. Chem. Soc. 89 (1967) 4809.